



Characteristics of Karst Formations and Their Significance for Shale Gas Exploration

Xiuquan Hu^{1,2}, Hong Liu^{1*}, Xiucheng Tan¹, Yong Dan³, Heng He⁴, Chenjing Xiao² and Ruixue Li²

¹School of Earth Science and Technology, Southwest Petroleum University, Chengdu, China, ²College of Energy Resources, Chengdu University of Technology, Chengdu, China, ³Institute of Karst Geology, Chinese Academy of Geological Sciences, Guilin, China, ⁴Chengdu Mianshi Foreign Language School, Chengdu, China

OPEN ACCESS

Edited by:

Shu Jiang,
The University of Utah, United States

Reviewed by:

Fei Ning,
Sinopec Petroleum Exploration and
Production Research Institute, China
Bo Peng,
Chinese Academy of Geological
Sciences (CAGS), China
Min Deng,
Chengdu Geological Survey Center,
China

*Correspondence:

Hong Liu
nd123@163.com

Specialty section:

This article was submitted to
Geochemistry,
a section of the journal
Frontiers in Earth Science

Received: 30 March 2022

Accepted: 25 April 2022

Published: 08 June 2022

Citation:

Hu X, Liu H, Tan X, Dan Y, He H, Xiao C
and Li R (2022) Characteristics of Karst
Formations and Their Significance for
Shale Gas Exploration.
Front. Earth Sci. 10:907685.
doi: 10.3389/feart.2022.907685

The classification method of karst formations is widely used in engineering and environmental geology but is seldom used in petroleum geology. In this study, the classification method of karst formations is applied to the sealing study of shale gas roof and floor carbonate rocks, and the influence on shale gas accumulation and drilling is discussed. The Paleozoic black shale in southern China is primarily formed by marine and transitional facies, and the intergrowth between shale and carbonate rocks is a basic geological feature of the Paleozoic strata in southern China. Carbonate karst is an unavoidable problem in shale gas exploration in southern China. Around the black shale target layer, in the Upper Paleozoic trait region, the study starts from the development strength of karst strata, through geological profile survey, spring flow statistics, test, and other methods and means; the shale and the carbonate rock contacted with it are taken as a whole to explore the impact of karst strata on shale gas drilling. The Upper Paleozoic karst strata in the study area were divided into two kinds, four types, and six subtypes. It was determined that the limestone continuous karst strata of the Sidazhai Formation and the second member of the Nandan Formation are the sensitive layers of shale gas drilling, whereas the first number of Nandan and Wuzhishan formations are shale reservoir-forming packers. In addition, a method for evaluating the karst sensitivity of shale gas exploration is summarized. The karst avoidance, karst-sensitive, and karst-insensitive areas for shale gas exploration were divided. Combined with the surface and underground conditions and the basic geological conditions of shale gas not being significantly different, shale gas drilling should avoid the fold core and fault zones.

Keywords: shale gas, karst drilling accident, shale roof and floor, karst formation, karst-sensitive area

INTRODUCTION

Shale gas is an unconventional oil and gas resource and a hotspot in global energy research (Liss 2014; Jia et al., 2016; Ma et al., 2018; Ma and Xie, 2018; Sarkar et al., 2018; Zhang et al., 2020a). It has low porosity and permeability and contains coexisting free gas and adsorbed gas (Wang et al., 2016; Zhang et al., 2022b). Shale gas exploration and development are currently being carried out by advanced technology in the United States and Canada (Soeder 2018; Ladevèze et al., 2019; Li et al.,

2020; Fahad et al., 2021); although the research, exploration, and development of shale gas in China have started not long time ago, a significant progress has been made in the shale exploration technology (Jiang et al., 2012; Zou et al., 2015, Zou et al., 2016; Fang 2019; Liang et al., 2020; Du et al., 2021; Gao et al., 2021; Zhang, et al., 2022a). Studies on shale gas have focused on the Sichuan Basin (Liu and Wang, 2016; Li et al., 2017; Liu et al., 2017; Zeng et al., 2018), and relatively little research has been conducted in southern Guizhou. With further research, scholars believe that the Jiusi, Liangshan, and Longtan Formations are the three main targets for shale gas formations in southern Guizhou (Tang et al., 2014; Zhang et al., 2016). The shale of the Huohong and Dawuba Formations of the Upper Paleozoic has high organic matter content and wide distribution, which is a shale gas target with great exploration potential in the southern Guizhou area (Miao 2018; Yuan et al., 2018).

In karst areas, drilling risks are high, and karst geological problems are prominent. In recent years, drilling and construction problems, such as cavitation, leakage, mud overflow, and other phenomena and even shut-in and abandoned wells have occurred several times. The Paleozoic strata in southern China are mainly formed by marine and transitional facies, and the mutual development between shale and carbonate rocks is the basic geological feature of the Paleozoic strata in southern China (Ma et al., 2011; Dan et al., 2013). Carbonate karst is an unavoidable problem for shale gas exploration in southern China, and karst poses a significant challenge for drilling in southern China. The classification method of karst formations is widely used as an important measure to study carbonate karst in engineering and environmental geology but less in petroleum geology. Karst formations focus on the thickness ratio and continuous thickness of rock strata and their combinations to reflect the karst development intensity and water-bearing and permeability characteristics of carbonate rocks. This is different from chronostratigraphy and biostratigraphy. It is also different from the general rock stratigraphic units of the Comprehensive Group of Projects on the Prediction, Utilization, and Management of Karst Groundwater Resources and Karst Water in the Dashui Mining Area in North China (1991). The combination types formed by carbonate rocks of different lithologies form the basis of the karst types. According to the statistics of the combination characteristics, thickness ratio, and continuous thickness of rock strata of different composition and structure types, the type of karst formations adopts the three-level classification method, and the first level of karst formations is divided by group statistics. The second class of karst formations is divided by segments: classification of the tertiary “subtype” of karst formations in lithological sections (Dan et al., 2015). Previous studies have classified the carbonate karst formations in the Halahatang region of Xinjiang (Dan et al., 2015).

The sedimentary environment of the black shale in southern Guizhou is relatively deep, and shale gas accumulation is closely related to carbonate rocks. Therefore, it plays an important role in selecting shale gas accumulation, drilling location, and drilling prevention measures to clarify the degree of development and spatial distribution of the top and bottom carbonate karst

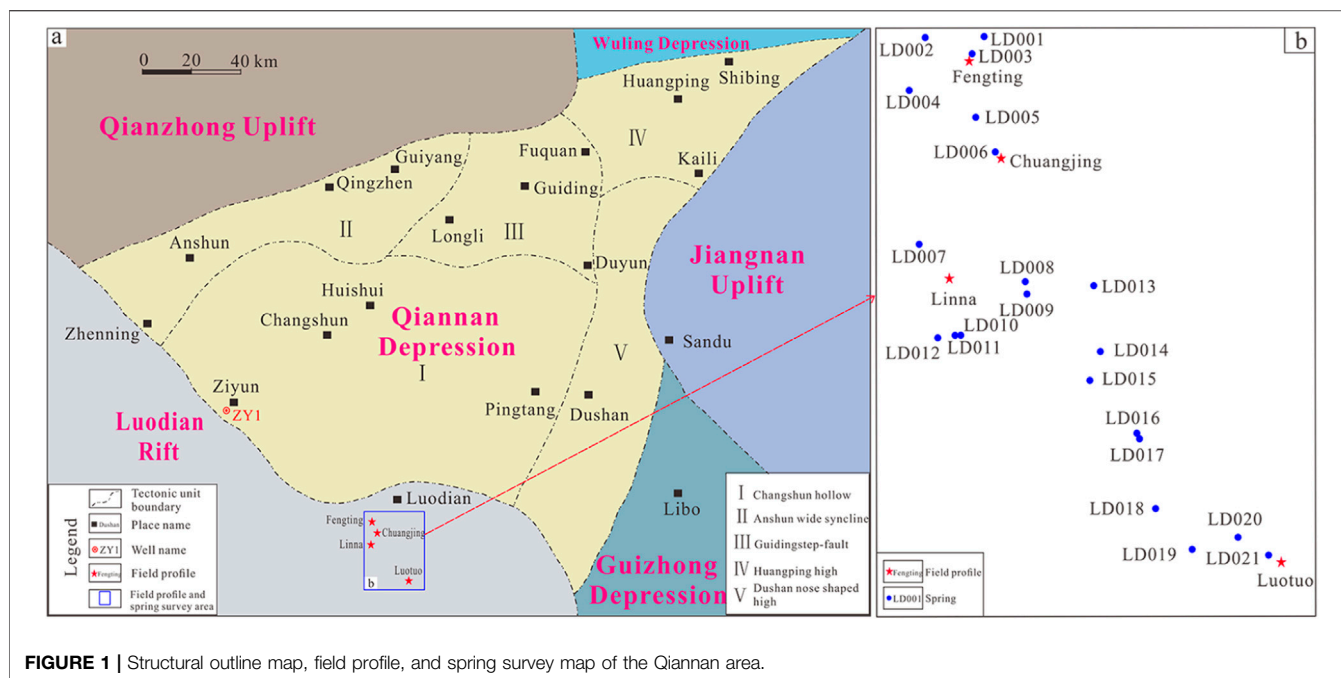
formations in the study area in contact with the shale gas target strata. Previous studies on shale gas in southern Guizhou mainly focused on the search and evaluation of shale gas target formations, and few studies analyzed the shale gas target formation and carbonate rocks in contact with it as a whole. To understand the influence of karst development in shale gas exploration, this study focused on field profiles, sample tests and analyses, spring surveys, and comprehensive surface and underground conditions (geophysical interpretation). For this study, we considered the target layer of shale gas in southern Guizhou and the carbonate rocks in contact with it as a whole, and the Upper Paleozoic carbonate rocks are divided according to the idea of karst formation. The karst development of carbonate rocks in the shale gas cap and floor was evaluated, and its influence on shale gas accumulation and drilling was discussed.

GEOLOGICAL BACKGROUND

The southern Guizhou Depression is located southeast of Guizhou and tectonically on the southwest margin of the Yangtze continental block. It is a residual ocean basin formed after multi-stage basin-forming sea-land conversion and is triangular in-plane (Xu et al., 2010; Zhang 2010) (**Figure 1**). It is adjacent to the Jiangnan uplift in the east, central Guizhou uplift in the northwest, Luodian Fault Depression in the southwest, and Guizhong Depression in the southeast. The southern Guizhou Depression experienced multi-stage tectonic movement, and the Caledonian stage was a relatively stable developmental stage of the Yangtze platform, which deposited a set of platform facies carbonate rocks. The Hercynian period is the development stage of the fault depression and the main forming stage of the southern Guizhou Depression. The Indosinian period was a period of depression development, while the Indosinian Movement ended the marine sedimentary history in the region (Mao et al., 1999; Wu 2003). The southern Guizhou Depression is based on the late Proterozoic metamorphic rock series, the sedimentary cover is Sinian–Triassic, and the surface outcrops change from old to new from east to west.

ANALYTICAL METHOD

Based on the field shale-karst geological survey and the test and analysis of samples, this study analyzed the geological characteristics of shale strata, such as lithology, organic carbon content, and vitrinite reflectance, and divided karst formations into kinds, types, and subtypes. Combined with the statistics of the number of fractures and caves in the field, the number of spring points, the flow rate of spring points, the development characteristics of karst formations in the study area, and the shale-related carbonate rocks are described in detail, and the karst-sensitive strata and favorable intervals are divided. An evaluation method for karst sensitivity in shale gas exploration is proposed based on surface and underground conditions (geophysical interpretation). In case there is an insignificant difference in the basic geological conditions of shale



gas, the avoidance zone for the deployment of shale gas drilling is proposed in the study area.

We conducted a systematic field study of the Upper Paleozoic section in the southern Guizhou area and observed three field sections (Chuangjing, Fengting, and Linna of Luodian), 21 spring points, and 19 large karst caves in detail, as well as one drilling core (Well ZY1). On this basis, systematic sampling was conducted, and 36 shale samples were selected, including 15 from the first member of the Huohong Formation, seven from the third member of the Huohong Formation, eight from the Dawuba Formation, and six from the upper part of the first member of the Nandan Formation of the Upper Carboniferous. A total of 36 shale samples were tested and analyzed for organic carbon content and vitrinite reflection. The samples selected include eight limestone samples, two lenticular limestones of the Wuzhishan Formation, two flinty limestones of the first member of the Nandan Formation, three limestone conglomerates of the second member of the Nandan Formation, and one micritic limestone of the Sidazhai Formation. Eight limestone samples were identified using thin-section identification and pore permeability tests. The experimental data in this study were obtained from the State Key Laboratory of Oil and Gas Reservoir Geology and Exploitation at the Chengdu University of Technology. The laboratory was established in 1990 with the approval of the National Planning Commission of China and the National Education Commission of China and passed the evaluation of the National Laboratory with good results in 2000, 2005, and 2010.

RESULTS

Analysis Results of Shale Samples

The samples collected were mainly black shale from the Upper Paleozoic. According to the field investigation, black shale mainly

developed in the first member of the Middle and Lower Devonian Huohong formations ($D_{1-2}h^1$), the third member of the Huohong Formation ($D_{1-2}h^3$), the Lower Carboniferous Dawuba Formation ($C_{1-2}dw$), and the upper part of the first member of the Upper Carboniferous Nandan Formation (CPn^1) (Figure 2). The first ($D_{1-2}h^1$) and third members ($D_{1-2}h^3$) of the Huohong Formation are a set of semi-bathyal or platform sedimentary facies mainly composed of gray-black claystone, limestone, and marl, containing slab stones and planktonic ostracod fossils. The formation thicknesses of $D_{1-2}h^1$ and $D_{1-2}h^3$ were 165–196 m and 72–85 m, respectively. The second member ($D_{1-2}h^2$) of the Huohong Formation is thick quartz sandstone with a thickness of 60–90 m. The lithology of the Dawuba Formation ($C_{1-2}dw$) is black shale, yellow-brown shale, sand shale, and calcareous shale with thin siliceous rock, sandstone, siliceous shale, and iron-bearing nodules, often with limestone and argillaceous limestone in the upper part, with thicknesses of 378–411 m. The first member of the Nandan Formation (CPn^1) is a platform basin to slope facies, which is integrated into the thin-medium thick siliceous layer of the Dawuba Formation. The lithology is mainly flinty limestone mixed with shale and siliceous rock, of which shale primarily exists in the upper part, and limestone mainly exists in the lower part with a thickness of 21–274 m. The second member of the Nandan Formation (CPn^2) is mainly composed of medium-thick micritic limestone and bioclastic micritic limestone, with almost no shale or siliceous rocks, and the stratum thickness is 283–559 m (Table 1).

The total organic carbon content (TOC) can reflect the amount of organic matter in shale, which is usually used to measure the abundance of organic matter and is also a key parameter for evaluating the hydrocarbon generation capacity of shale (Zhao et al., 2021). Vitrinite reflectance (R_o) is often used as an effective indicator to determine the degree of thermal evolution in source rock

TABLE 1 | Stratigraphic division table of Upper Paleozoic in the Qiannan area.

System	Series	Formation (Member)	Thickness(m)	Lithology	
Permian	Upper	Linghao Formation	Third member	106–194	Interbedded thin to middle-thick layers of siltyclaystone and tuffaceous siltstone
			Second member	124–368	Thick and massive tuffaceous siltstone and argillaceous siltstone, intercalated with a small amount of medium thick tuffaceous sandstone
			First member	111–172	Interbedded thin to middle-thick layers of tuffaceous siltstone, fine sandstone and siltyclaystone
	Middle	Sidazai Formation	Second member	238–735	Interbedded thin to middle-thick flinty limestone and bioclastic limestone
			First member	8–169	Interbedded thin-layered siliceous rock, argillaceous siliceous rock and siltyclaystone, intercalated thin-layered flint-stripped limestone
	Lower				
Carboniferous	Upper	Nandan Formation	Second member	283–559	Thin to middle thick layers of chert-bearing micrite limestone, bioclastic, with a small amount of thin siliceous rocks
			First member	21–274	Thin to middle layer of chert-bearing micrite limestone intercalated with siliceous rock and carbonaceous shale, of which shale mainly exists in the upper part and limestone mainly exists in the lower part
	Lower	Dawuba Formation		378–411	Thin to middle shale, silty shale, calcareous shale intercalated with thin layered siliceous rock, sandstone
Devonian	Upper	Wuzhishan Formation		30–186	Lenticular limestone, clastic limestone and argillaceous banded limestone
		Liujiang Formation		77–113	The lower part is clay siliceous rock and the upper part is siliceous shale
	Middle	Huohong Formation	Third member	72–85	Middle-thick layer claystone, siltyclaystone, and interbedded organic claystone
			Second member	60–90	Thick and massive fine-grained quartz sandstone, quartz siltstone, locally intercalated with a small amount of shale
	Lower		First member	165–196	Middle-thick layer claystone, siltyclaystone, and interbedded organic claystone

reservoirs. According to the classification standard for the maturity stage of black shale in South China, $R_o < 0.5\%$ is immature, $0.5\%–1.3\%$ is mature, $1.3\%–2.0\%$ is highly mature, and $2.0\%–3.0\%$ is early over-mature. It is also observed that $3.0\%–4.0\%$ is in the late over-mature stage, whereas R_o over 4.0% is in the metamorphic stage (Zhang, et al., 2020b; Zhao et al., 2021). According to measured organic geochemical data, the organic carbon content of shale in southern Guizhou is between 0.2% and 4.5% , and the organic carbon content is relatively high in general. The maximum organic carbon content of 4.5% occurs in the first member of the Huohong Formation (Figure 3). The organic carbon content of the samples measured in the first section of the Huohong Formation was 1.04% , that of the third section of the Huohong Formation was 1.48% , that of the Dawuba Formation was 1.52% , and that of the first section of the Nandan Formation was 2.51% . According to the vitrinite reflectance (R_o) test data of the shale, the lowest value was 3.0% , which occurred in the first member of the Huohong Formation, and the highest value was 5.1% , which occurred in the first member of the Huohong Formation and the first member of the Nandan Formation. Overall, the R_o of the shale in each group ranged from 3.0% to 5.1% , which is in the stage of over maturity and metamorphism, with little difference among the groups (Figure 4).

Classification of Karst Formations

The shale-related carbonate rocks in the study area mainly include marl of the Wuzhishan Formation (D_3wz), limestone of CPn^2 , and flinty limestone of the Sidazhai Formation (P_{1-2s}). Considering these three sections as the key research layers, the karst formations in the study area can be divided into two kinds (homogeneous pure carbonate rock and heterogeneous carbonate rock), four types (the

carbonate continuous type, clastic rock and carbonate rock interbed type, clastic rock intercalated with carbonate rock type, and carbonate rock intercalated with clastic rock type), and six subtypes (micrite, crystalline grain limestone subtype, the chert limestone subtype, the argillaceous band limestone subtype, the shale and limestone interbed type, shale intercalated with limestone subtype, and limestone intercalated with shale subtype) (Table 2).

Based on previous research results (Dan et al., 2015), combined with the lithology, thickness ratio, continuous thickness, and combination form of the study area, the karst formations of the Upper Paleozoic carbonate rocks in southern Guizhou are classified. The strong karst formations are carbonate continuous-grain stone subtypes, and the strata are the second member of the Nandan Formation. The medium-strong karst formations belong to the carbonate continuous-flinty limestone subtype, and the strata belong to the Sidazhai Formation. Weak-medium karst formations are carbonate intercalated with clastic rock, marl, and limestone intercalated with mudstone, and the strata are the lower part of the first member of the Nandan and Wuzhishan formations. The weakly karstified formations are clastic rock interbedded carbonate type-shale interbedded limestone subtype and clastic rock interbedded carbonate type-shale interbedded limestone subtype, and the strata are the first member of the Huohong Formation and the lower part of the first member of the Nandan Formation (Figures 5, 6).

Development Characteristics of Karst Formations

Karst-Fracture Characteristics

According to field investigations, thin section identification, and drilling core observations, there are no obvious dissolution pores



in the argillaceous limestone section of the Wuzhishan Formation or the interbedded section of flint limestone and shale in the lower part of CPn^1 , and fractures and interbedded surfaces are the main storage spaces. Karst caves and fractures are well-developed in the middle thick limestone continuous section of CPn^2 , but the dissolution pores are locally developed, and their distribution is extremely uneven. The continuous intervals of middle-layered limestone in the Sidazhai Formation are mainly composed of fractures and karst caves (Figure 7). The number of karst caves reflects the karst intensity of different strata on one side. In this study, the number of karst caves with widths greater than 40 cm was used in the field profile. We could have considered small karst caves with a width of less than 40 cm to be modern karst caves formed by near-surface carbonate rock strata being dissolved in a short duration, which is not representative; therefore, the number

was not counted. The data show that the karst caves in CPn^2 are the most developed, followed by those in P_{1-2s} , and the karst intensity is relatively strong. There were no large karst caves in D_3wz or CPn^1 , and the degree of karst development was relatively weak (Figure 8).

Spring Point and Flow Characteristics

The number of spring points and amount of discharge in different strata can also reflect the degree of development of karst fractures and underground rivers in the interior of the corresponding strata and the occurrence degree of groundwater. The investigation of 21 spring points on the surface of the study area shows that the spring points are exposed in several strata but mainly in the Sidazhai Formation (Figure 8). The number of spring points was 12, which is significantly higher than that of the other strata. The

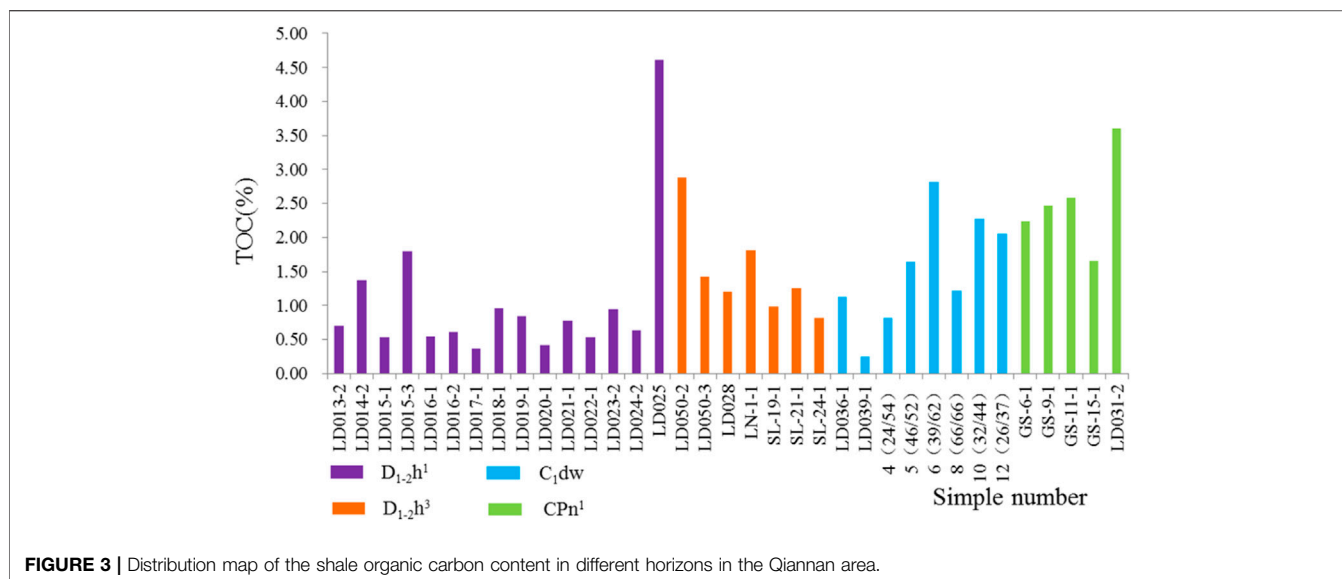


FIGURE 3 | Distribution map of the shale organic carbon content in different horizons in the Qiannan area.

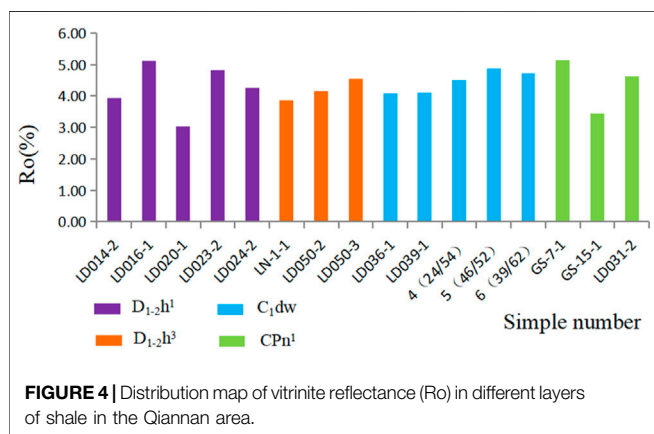


FIGURE 4 | Distribution map of vitrinite reflectance (Ro) in different layers of shale in the Qiannan area.

Nandan and Wuzhishan Formations are less exposed. There are also a few spring points exposed in the Huohong and Dawuba Formations of the shale. According to the statistics of the spring flow, the average flow rates of D₁₋₂h², D₃wz, and CPn² are less than 1 L/s. The average flow rate of CPn¹ was generally 4.7 L/s. The number of spring points in the Dawuba Formation is small, but the flow rate is high, reaching 21.21 L/s. The average flow rate of the Sidazhai Formation was the largest, reaching 29.31 L/s. However, the flow rate of the spring points in this stratum was significantly different, with the lowest of 1.11 L/s and the highest of 65.21 L/s. Overall, the Sidazhai Formation has a strong degree of karst development and abundant formation water; CPn¹ and CPn² have general karst development and underdevelopment of formation water; the Wuzhishan Formation suffers from weak karstification and underdevelopment of groundwater (Figure 8).

Physical Characteristics

The physical properties of limestone are closely related to lithology, which is the basis of other factors affecting the physical properties of limestone. The outcropping sample test

showed that the average porosity and maximum permeability of the lenticular limestone in the Wuzhishan Formation (D₃wz) were 1.50% and $0.0014 \times 10^{-3} \mu\text{m}^2$, respectively, and the average porosity and maximum permeability of the flinty limestone in the interbedded section between flinty limestone and shale in the Nandan Formation were 1.62% and $0.0015 \times 10^{-3} \mu\text{m}^2$, respectively. The limestone conglomerate porosity of CPn² was greater than 2.0%, with an average porosity of 2.09%. The minimum, maximum, and average permeabilities were $0.0005 \times 10^{-3} \mu\text{m}^2$, $0.0033 \times 10^{-3} \mu\text{m}^2$, and $0.0018 \times 10^{-3} \mu\text{m}^2$, respectively. The permeability of CPn² varies significantly. The average porosity of the middle-layered micritic limestone in the Sidazhai Formation (P₁₋₂s) was 1.33%, and the permeability was as low as $0.0011 \times 10^{-3} \mu\text{m}^2$ (Figures 9, 10). Overall, the physical properties of the CPn² limestone conglomerates were better than those of the D₃wz lenticular limestone, CPn¹ chert limestone, and P₁₋₂s micritic limestone.

Division of Karst Sensitive Layer and Favorable Interlayer

The study area was mainly deep-water and semi-deep water environments from the Devonian to Permian. The lenticular limestone of D₃wz and Devonian and the flinty limestone of CPn¹ and Upper Carboniferous have a stable regional distribution with a thickness of 50–100 m and poor physical properties of the main rock matrix. The average porosity of the lenticular limestone of the Wuzhishan Formation was 1.5%, and the maximum permeability was $0.00144 \times 10^{-3} \mu\text{m}^2$. The average porosity and permeability of the CPn¹ flinty limestone were 1.629% and $0.0015 \times 10^{-3} \mu\text{m}^2$, respectively; the layer between the surface and fracture was the storage space. The water distribution was weak, and the ancient water system was relatively undeveloped. Groundwater discharges into the deep part of the lower stream river through interlayers or fault runoff. No karst caves were found in the two layers, and there were fewer

TABLE 2 | Classification table of carbonate karst formation types in the Qiannan area.

Kind	Type	Subtype	Stratum	Lithological characteristics	Karst formation classification
Non-homogeneous carbonate rocks	Carbonate rock intercalated with the clastic rock type	Limestone intercalated with shale subtype	First member of the Nandan Formation	Medium-thick micrite limestone intercalated with thin shale	Weak-medium karst formation
	Clastic rock intercalated with carbonate rock type	Shale intercalated with limestone subtype	First member of the Huohong Formation, the lower part of the first member of the Nandan Formation	Medium-thick shale intercalated with thin marl	Weak karst formation
	Interbedded clastic rock and carbonate rock type	Interbedded subtypes of shale and limestone	Lower part of the first member of the Nandan Formation	Interbedded medium-thin shale and micritic limestone	Weak-medium karst formation
Homogeneous Pure Carbonate Rocks	Continuous carbonate rock type	Subtypes of micritic and silty granular limestone	Second member of the Nandan Formation	Middle-thick layer of powder grain limestone, locally intercalated with a middle-thick layer of micrite and powder crystal limestone	Strong karst formation
		Flinty limestone subtype	Sidazhai Formation	Continuous distribution of middle-thin layers of flinty limestone	Medium-strong karst formation
		Subtype of argillaceous banded limestone	Wuzhishan Formation	Middle-thin argillaceous banded limestone, lenticular limestone, and nodular limestone	Weak-medium karst formation

springs and a lower average flow. The spring point survey in the Wuzhishan Formation discovered a spring where the average flow rate is 0.8 L/s, and three spring points found in the CPn¹ had an average flow rate of 4.7 L/s. The surface does not form a typical karst landform. Therefore, the comprehensive study indicates that the lenticular limestone of D₃wz and the flinty limestone of the CPn¹ of Upper Carboniferous are weak-medium karst formations.

There is a layer of 20–50 m argillaceous limestone in the middle of the Upper Carboniferous–Lower Permian (including CPn² and P_{1-2s}), and the rest are continuous middle-thick limestone. The total thickness of the limestone is greater than 800 m, and the hydrodynamic conditions are good, especially by dissolution and erosion. The paleo-drainage system is developed, and the water-bearing capacity is strong; therefore, it is a regional aquifer. In the Upper Carboniferous–Lower Permian carbonate distribution area on the surface, karst peak clusters were formed on the landform, with large surface height differences and relatively high physical properties of the bedrock. For example, the average porosity of CPn² was 2.09%, and the average permeability was $0.0018 \times 10^{-3} \mu\text{m}^2$. The karst is well-developed. There were 15 karst caves with widths larger than 40 cm in the CPn² field profile and four karst caves with widths larger than 40 cm in the P_{1-2s} field profile. In addition, there were 12 spring points in P_{1-2s}, and the average flow rate could reach 29.3 L/s. Therefore, a comprehensive analysis showed that CPn² and P_{1-2s} are medium-strong karst strata. However, lithological differences existed between CPn² and P_{1-2s}. The lithology is the basis of karst development. The higher the purity of carbonate rock (i.e., the higher the content of calcite (CaCO₃)), the better is the karst development, the larger is the karst space formed, and the stronger is the water-rich capacity (Huang 2012). Inhomogeneous carbonate rocks contain insoluble minerals, such as argillaceous, siliceous, and carbonaceous minerals that fill karst fractures, making it difficult for groundwater to pass

through and weak karst development (Karst Research Group, Institute of Geology, Chinese Academy of Sciences 1979). Predecessors in the Ordovician rocks of the Tarim Basin for the dissolution test showed that when the noncarbonate composition (approximately equal acid insoluble content) is below 10% and had no significant effect on karstification, the relative dissolution rate was slightly higher than that of pure calcite high at 1.01–1.06. When the noncarbonate composition increased, karstification was abate, and the analysis of rock soluble was as follows: pure granular limestone > dolomitic limestone > dolomite > marl. The relative dissolution of different rocks forms the basis for the classification of the relative karst strength of different layers (Dan et al., 2015). CPn² is mainly composed of medium-thick powder crystal granular limestone and is partially intercalated with medium-thick micritic limestone. The Sidazhai Formation continuously distributes medium-thick flinty limestone, which is less soluble than the CPn² powder crystal granular limestone, and the number of karst caves is not as good as that of CPn².

Comprehensive analysis showed that the lenticular limestone of D₃wz and flinty limestone of CPn¹ are weak-medium karst formations, which are favorable barrier layers for shale gas exploration. The powder crystal granular limestone of CPn² and the flinty limestone of P_{1-2s} are high karst formations and sensitive strata for shale gas exploration, which are prone to karst geological problems and are not conducive to shale gas drilling.

DISCUSSION

Influence of Karst on Shale Gas Accumulation

The southern Guizhou area is a high- and steep-fold area with a large dip angle and well-developed faults. In the field investigation of the carbonate shale formation, it was found

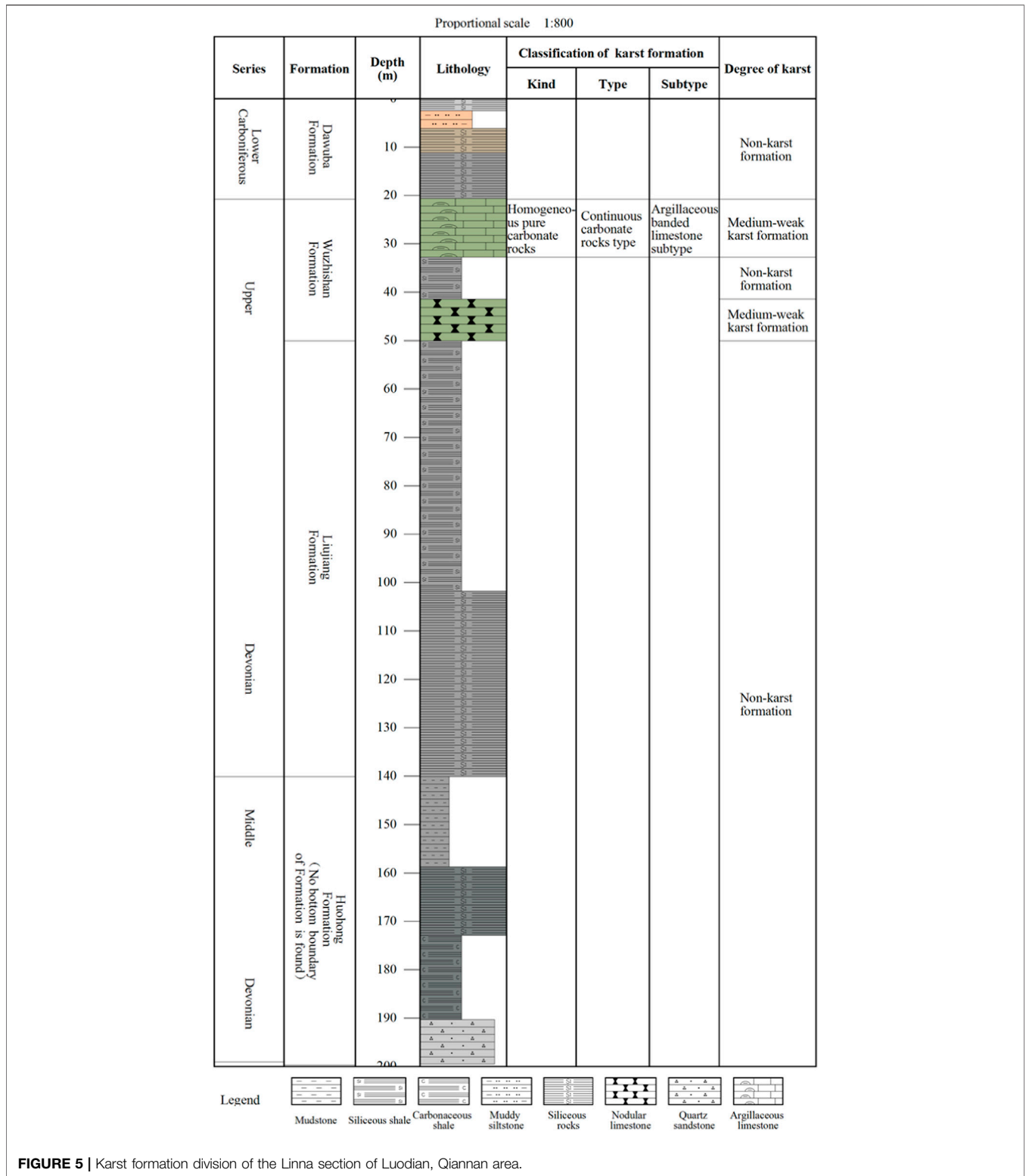


FIGURE 5 | Karst formation division of the Linna section of Luodian, Qiannan area.

that there is interbedded siliceous limestone in the upper part of the shale of the Dawuba Formation and marl in the lower part of the Wuzhishan Formation. The shale of the Devonian Huohong Formation is directly overlain by the siliceous rock

of the Liujiang Formation and the lenticular limestone of the Wuzhishan Formation, forming several sets of vertically interbedded marl and shale, with a good gas containment system.

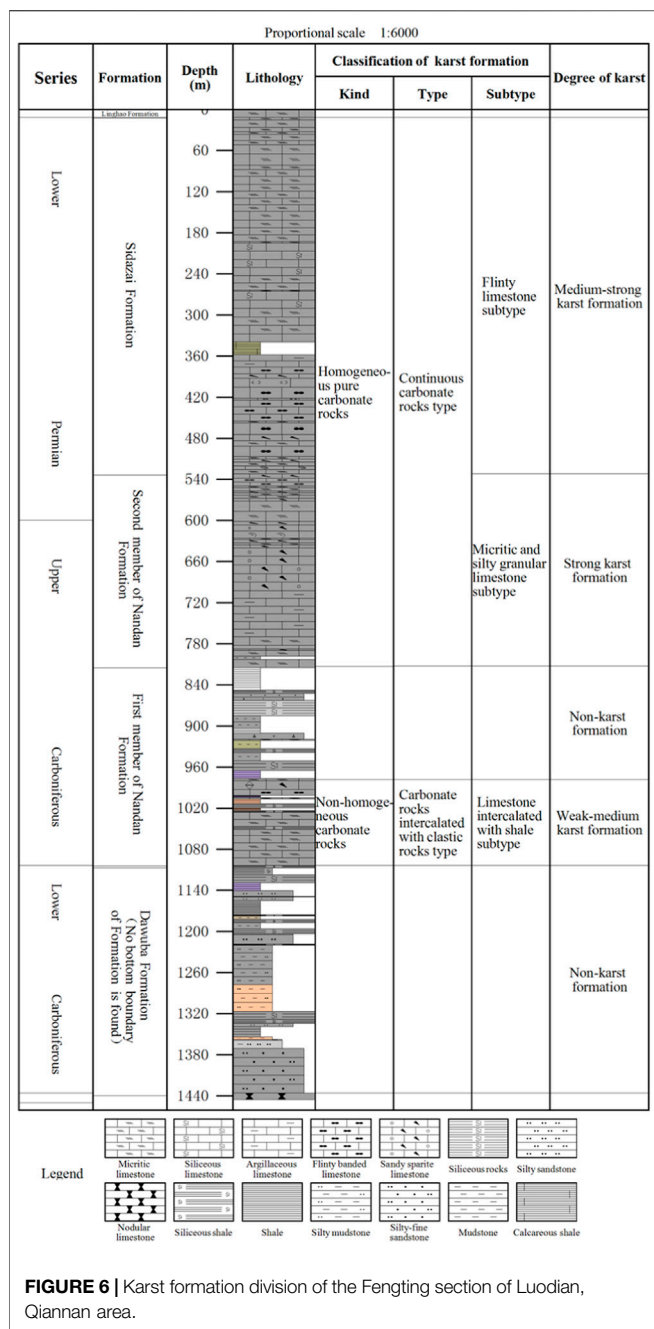


FIGURE 6 | Karst formation division of the Fengting section of Luodian, Qiannan area.

Owing to the structural damage, the formation was severely transversely damaged by faults and folds. Therefore, it is necessary to identify areas with relatively weak structural failure and effective isolation of shale by marl. Through detailed field observations (Figure 11), it was found that in the extrusion background, the stress was largest in the fold core, forming more kneading and fractures. In this high-stress background, marl and shale will produce a large number of fractures; therefore, shale gas will be dispersed under this condition. However, the wing situation was different. The structural stress on the wing was relatively weak, and the fractures were less developed. Generally, the micro-fractures in the shale will not pass through the marl, which can form a good

isolation system, and the probability of leakage occurring when drilling in karst aquifers is correspondingly smaller. In conclusion, for the southern Guizhou region, the fold core is proposed to be the avoidance area for shale gas drilling, and the fold wing is the potential enrichment area for shale gas (Figure 12).

Influence of Karst Formations on Drilling and Fracturing of Shale Gas Wells

Paleozoic carbonate rocks are well developed in China. Large sets of carbonate rocks developed laterally at the top and bottom of the shale, and carbonate interlayers were also present in the local shale layers. Overall, the ratio of the thickness of Paleozoic carbonate to shale is greater than 3:1 in southern China. However, the development of large carbonate rocks causes several problems during shale gas drilling. For example, when drilling a well ZY1 in Ziyun County, Guizhou province, to a depth of 374 m, drilling fluid appeared in a natural cave approximately 150 m away from the wellhead center, and leakage occurred when drilling 451 m deep. This is because the Permian Sidazhai Formation in the well is a medium-strong karst layer group, rich in groundwater, belonging to the confined water layer, and the upper clastic rocks of the Permian Wujiaping Formation, 337 m–372 m, are waterproof layers of the confined water layer. When drilling through the waterproof layer, the drilling fluid rises and communicates with the surface water through the underground leakage section (50 m deep), causing surface pollution. In view of the karst accident in the ZY1 well, the follow-up treatment measures of drilling through the water layer and sealing the water layer with casing were carried out. It was found that the overflow was obviously stopped after sealing the water layer, which reduced the risk of the next construction. Therefore, when selecting the well location, it is necessary to analyze the development degree of the karst layer group in the drilling area in advance and avoid medium-strong karst formations as far as possible. In addition, it is necessary to analyze the development, distribution, and tectonic stress environment of karst aquifers to take countermeasures in advance when drilling.

Fracturing is an important technical step in establishing efficient and economic developments of shale gas (Yu et al., 2022). Different types of carbonate karst formations exhibit different fracturing responses to the shale. When carbonate and shale with good physical properties are mutually developed, if the fracturing and completion method of late shale is not properly chosen, the water in the aquifer may enter the shale gas layer, resulting in an increase in water production and a decrease in gas production in shale gas wells. However, the fracturing fluid may escape from the overlying porous carbonate aquifer and pollute the groundwater. For example, CPn² and P₁₋₂s above the upper shale of CPn¹ belong to the strong karst formations. When fracturing the upper shale of CPn¹, energy is easily lost, and the fracturing fluid can easily enter the confined water layer of the second member of the Nandan and Sidazhai Formations, causing pollution. Carbonate rock strata with poor physical properties, poor porosity, and permeability (such as marl interlayers) act as fracturing barriers in fracturing so that hydraulic fracturing

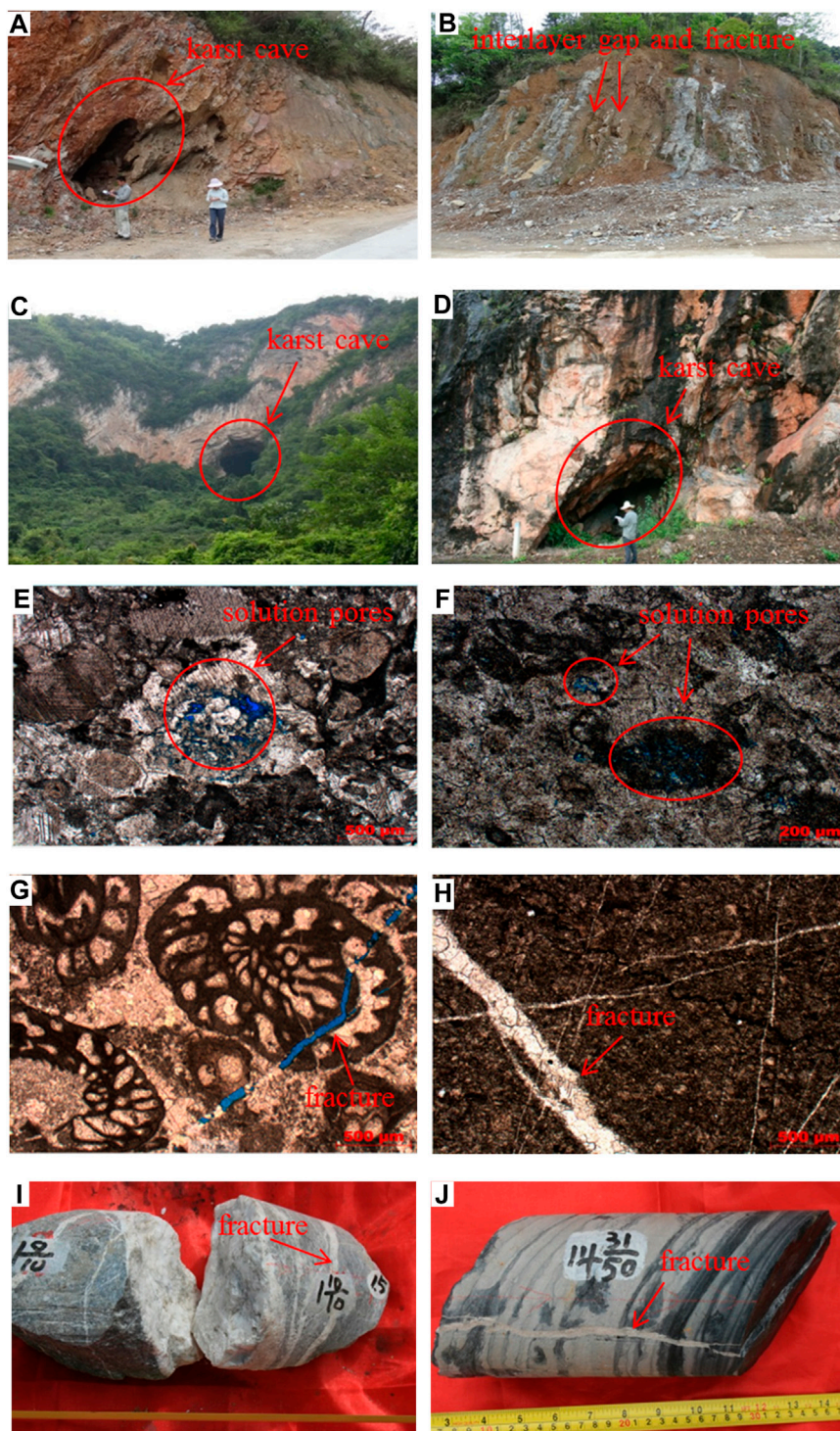
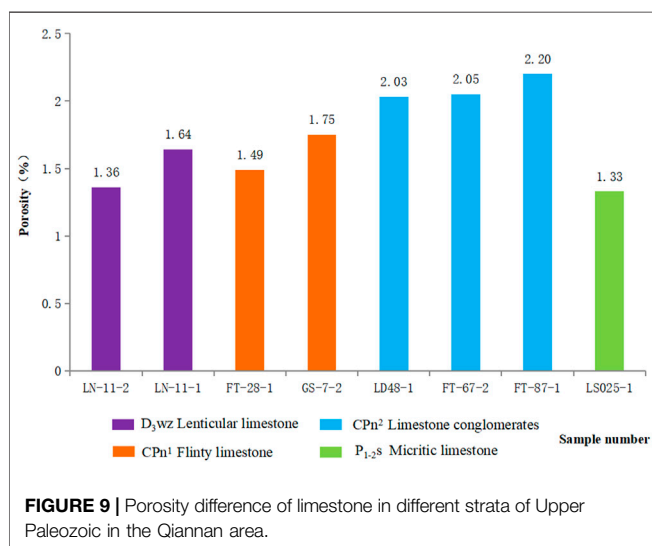
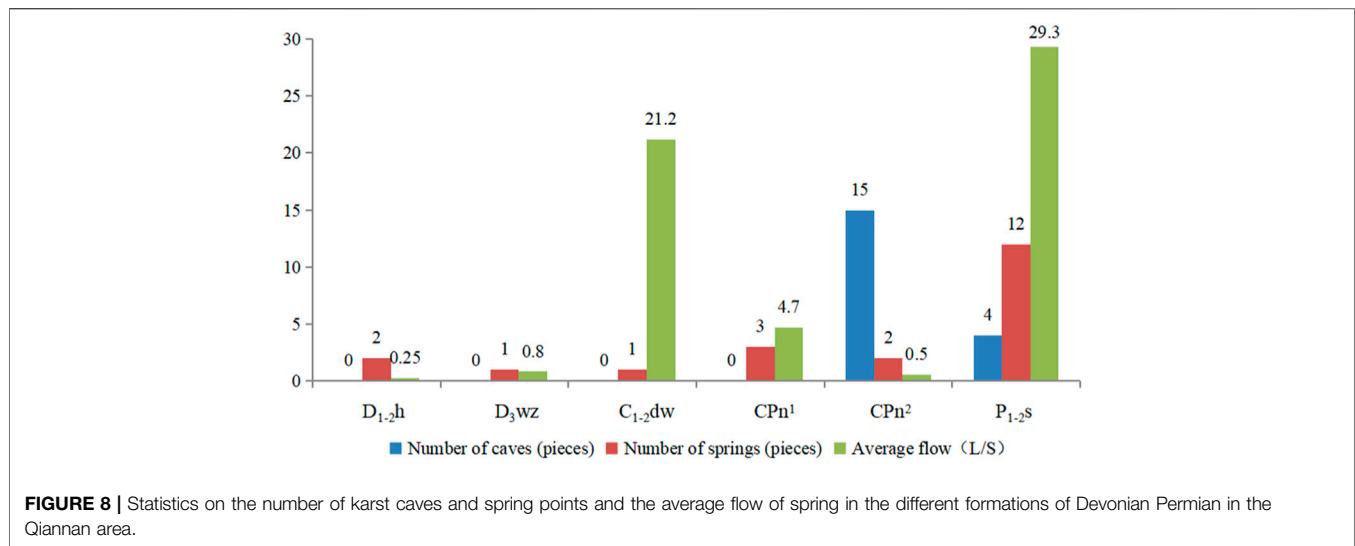


FIGURE 7 | Reservoir space types of different karst formations. **(A)** Karst caves are developed in CPn^2 (Fengting section in Luodian). **(B)** Marl of the Wuzhishan Formation. Reservoir space is the interlayer gap and fracture (Fengting section in Luodian). **(C)** Karst caves are developed in CPn^2 (Luotuo section in Luodian). **(D)** Karst caves are developed in CPn^2 (Mengjiang Bridge in Luodian). **(E)** Limestone with solution pores of CPn^2 (Fengting section in Luodian). **(F)** Limestone with solution pores of the Sidazhai Formation (Fengting section in Luodian). **(G)** Limestone of CPn^2 , fracture growing (Fengting section in Luodian). **(H)** Limestone of CPn^2 , fracture growing (Fengting section in Luodian). **(I)** ZY1 limestone of CPn^2 , fracture growing (well ZY1); **(J)** Marl of the Wuzhishan Formation, fracture growing (well ZY1)



cracks stop under the marl barrier, resulting in high shale gas exploitation efficiency (Dan et al., 2018). For example, the shale of the Huohong Formation is covered by a weak karst layer of the Wuzhishan Formation, and the energy generated by hydraulic fracturing can be preserved in the target shale gas layer, which is beneficial for producing complex artificial fracture networks and improving shale gas production.

Evaluation of Karst Sensitivity in Shale Gas Exploration

In recent years, many karst geological problems have appeared during shale gas drilling in southern China. For example, in 2013, Sinopec drilled karst caves at a depth of 15 m in the DY1 HF well of the Dingshan structure, and repeated leakages led to more than 22 days of pipe construction. In 2015, when drilling an HD1 well to a depth of 800 m in a shale gas well around the Yangtze River in

Guangxi, the China Geological Survey encountered a large amount of mud leakage, and drilling could not be conducted. The wellhead was then moved 5 m away, and 800 m was drilled again. In 2017, in the shale gas risk exploration well ZY1 in Ziyun County, Guizhou province, karst problems occurred on the surface and deep, resulting in well leakage. To avoid construction problems such as drilling emptying, leakage, mud overflow, shut-in, and waste wells, karst sensitivity evaluation of shale gas exploration should be conducted before shale gas drilling construction.

In actual exploration and development, whether on the surface or underground, drilling success is directly related to the degree of karst development. Therefore, in the evaluation of the karst sensitivity of shale gas exploration, the degree of difficulty in shale gas exploration and development should be evaluated by combining the surface and underground conditions. The surface conditions include the surface lithology and karst formation characteristics, topography and geomorphology, well site water supply conditions, and karst pipeline development. Underground conditions include karst aquifer development, fold location, distance from the fault zone, hydrodynamic conditions, and karst geophysical exploration (Table 3).

According to the aforementioned evaluation indices, the karst sensitivity of shale gas exploration in the study area was evaluated, which was divided into karst avoidance, karst-sensitive, and karst-insensitive areas (Figure 13). The avoidance area was mainly distributed near the fault and widely distributed throughout the entire area. It was distributed in the northern, central, and southern parts of the study area. Since the exposed surface strata are the middle-strong karst strata of CPn² and P₁₋₂s, a karst landform is developed, and the fracture karst caves are widely distributed. The karst-sensitive area has a large distribution in the entire area. The surface-exposed stratum is the moderate karst stratum of CPn¹, and its dissolution strength is weak. It is mainly dominated by cracks and is at a certain distance from the fault zone. The karst-insensitive area is mainly distributed near Gongli village and Narao village in the northern region, sporadically distributed in the south,

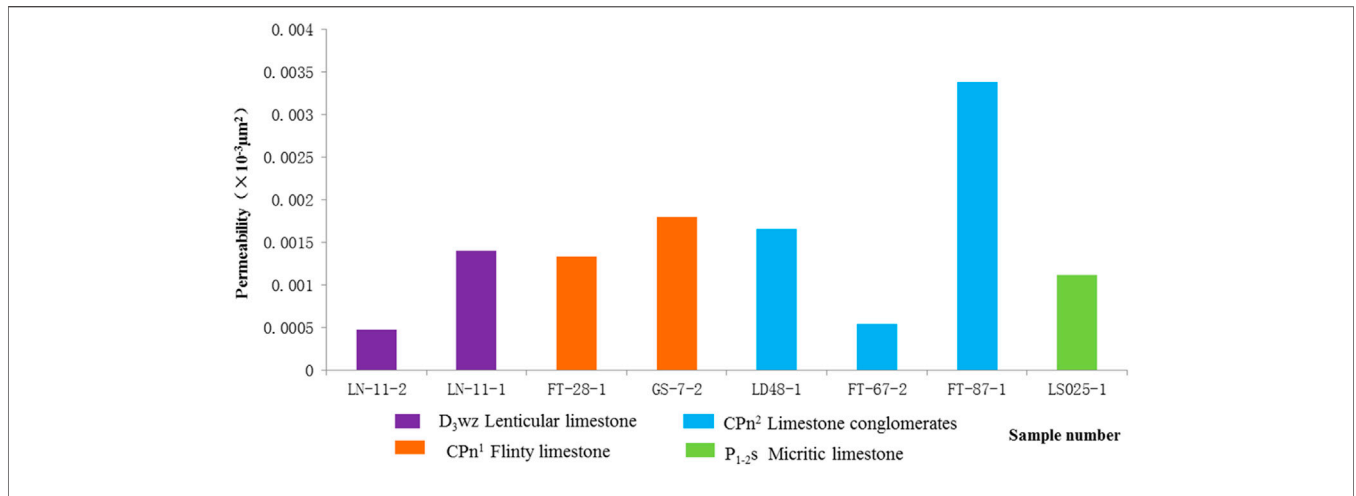


FIGURE 10 | Permeability difference of limestone in different strata of Upper Paleozoic in the Qiannan area.

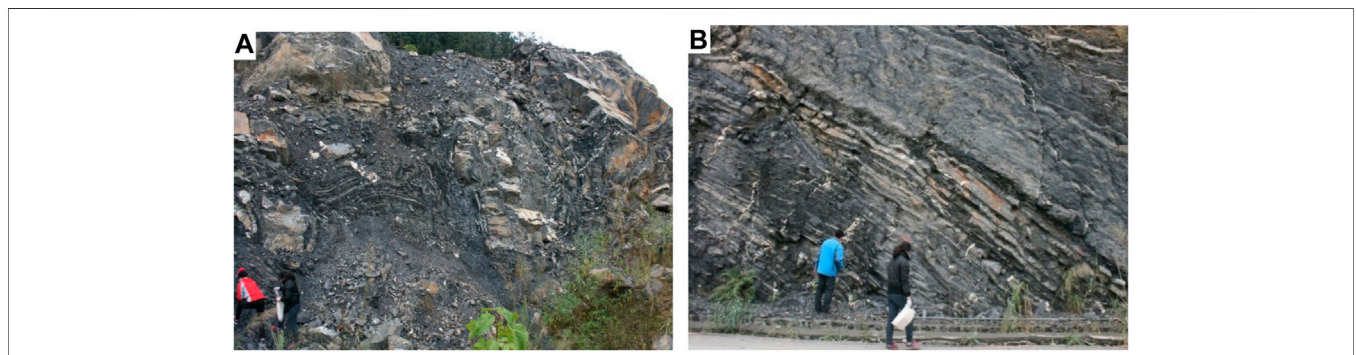


FIGURE 11 | Effectiveness of marl sealing in different structural parts. **(A)** Strongly folded marl destruction in the core of anticline, sealing failure. **(B)** Fractures in wing shale are interrupted in limestone and filled with calcite, sealing effective.

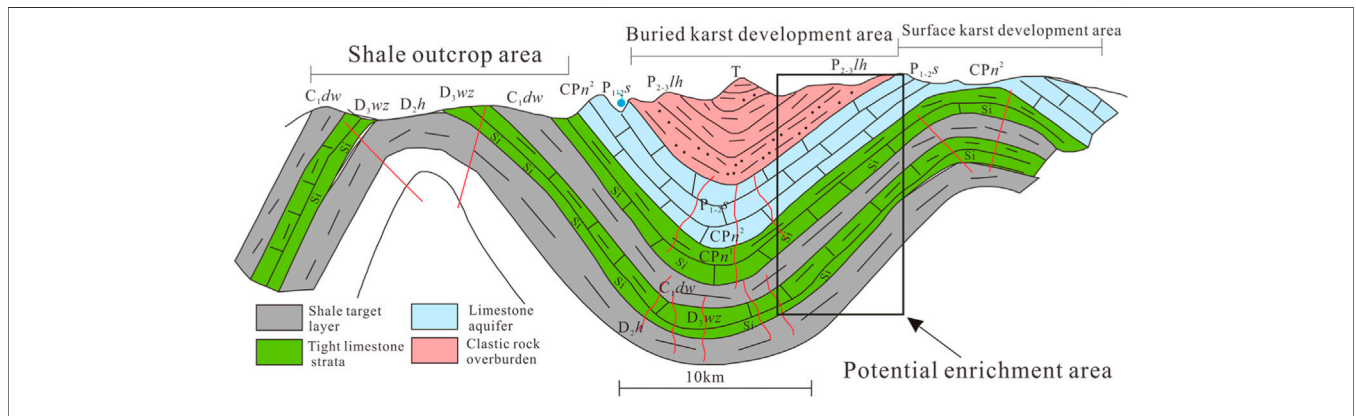


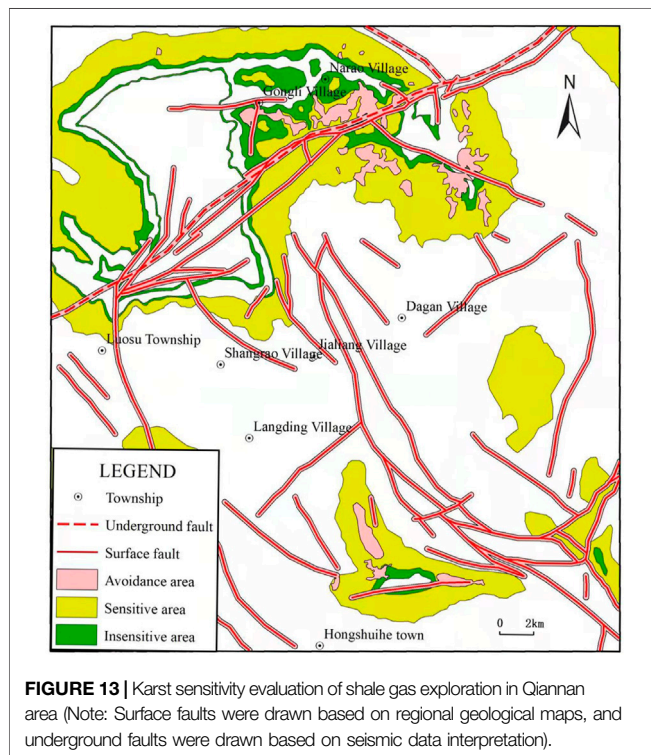
FIGURE 12 | Carbonate controlled shale accumulation model under complex tectonic background in the Qiannan area.

and far away from the fault zone as a whole. The surface is a clastic rock hilly landform with minimal undulation and abundant surface water.

Surface faults were drawn based on regional geological maps, and underground faults were drawn based on seismic data interpretation.

TABLE 3 | Division table of karst sensitivity evaluation for shale gas exploration.

Evaluation index		Karst avoidance area	Karst-sensitive area	Karst-insensitive area
Surface conditions	Surface lithology and characteristics of karst formation	Thick continuous limestone, dolomite, and strong karst formation	Middle or thick limestone, impure limestone development area, and medium-strong karst formation	Clastic rock area, clastic rock, clastic rock intercalated with carbonate rock, and weak karst formation
	Topography	Typical karst landform with large height difference relative to topography	Karst landform is developed, and the relative topographic height difference is larger.	Clastic rock hilly or mountainous landform, with little topographic fluctuation
	Water supply conditions of the well site	The groundwater table is deep, far from surface rivers.	The groundwater level is general, and the distance from the surface river is general.	The groundwater level is shallow and close to the surface river.
	Development status of karst pipeline	Underground rivers or caves are developed.	Underground rivers or karst caves may be developed.	No underground rivers or caves are developed.
Underground conditions	Development status of the karst aquifer	One or more sets of medium-strong karst aquifers (sensitive layers) are developed.	One or more sets of medium-strong karst aquifers or interbedded karst formations are developed.	Mainly clastic rocks, with little or no karst aquifers are developed.
	Fold position	Fracture development zone of the syncline core	Syncline core or wing	Syncline wing
	Distance from the fault zone	On the fault zone	Near the fault zone	Far away from the fault zone
	Hydrodynamic conditions	Deep circulation runoff-discharge area	Deep circulation runoff-discharge area	Deep circulation recharge area
	Geophysical prospecting for karst	Abnormal development zone	Abnormal development zone	Non-abnormal development zone



CONCLUSION

In this study, we discovered that it is feasible to apply the classification method of karst formation to the sealing study of carbonate rocks in the roof and floor contact with shale and further explore the influence on shale gas accumulation and

drilling, which is worthy of popularization and application in the field of oil and gas geology. The main target layers of black shale in southern Guizhou are $D_{1-2}h^1$ and $D_{1-2}h^3$ of the Middle-Lower Devonian, the $C_{1-2}dw$ of Lower Carboniferous, and the upper part of CPn^1 of the Upper Carboniferous. The carbonate rocks related to the shale target layer mainly include the D_{3wz} marlite of the Upper Devonian, CPn^2 limestone of the Upper Carboniferous–Lower Permian, and P_{1-2s} flinty limestone of the Middle-Lower Permian.

The carbonate karst formation in the Qiannan area can be divided into two types, four types, and six subtypes. Among them, CPn^2 and P_{1-2s} were mainly developed in the medium-thick layer and medium-bedded limestone. Corrosion cracks and corrosion holes and karst springs were developed. These are medium-strong karst formations and shale gas drilling-sensitive layers. The lenticular limestone of D_{3wz} and the flinty limestone of CPn^1 had poor matrix physical properties, and no karst caves were found in the survey. There were a few springs, and the average flow rate was low. These are the weak-middle karst formations and shale gas reservoir isolation layers.

The shale gas exploration avoidance area in southern Guizhou is mainly distributed near the fault, and the exposed strata are CPn^2 and P_{1-2s} ; the surface-exposed strata in the sensitive area are weakly medium karst formations in CPn^1 , and there is a certain distance from the fault zone. The karst-insensitive area is mainly scattered in the northern part of the study area and is far away from the fault zone as a whole.

Based on our results, we recommend that to avoid karst drilling accidents, shale gas drilling should avoid fold cores and fault zones under the condition that the basic geological conditions of shale gas are not significantly different, considering the surface and underground conditions.

DATA AVAILABILITY STATEMENT

The original contributions presented in the study are included in the article/Supplementary Material; further inquiries can be directed to the corresponding author.

AUTHOR CONTRIBUTIONS

XH, HL, XT, and YD contributed to the study's conception and design. XH wrote the first draft of the manuscript. HH, CX, and RL conducted the investigation and data collection. All authors contributed to the manuscript's revision and read and approved the submitted version.

REFERENCES

- China (1991). "Karst Strata Association Types of the Cambrian–Ordovician in North China and Regulation of Their Regional Variation," in *Karst China*, 29–38. Available at: <https://kns.cnki.net/kcms/detail/detail.aspx?FileName=ZGYR199102003&DbName=CJFQ1991>.
- Dan, Y., Liang, B., Cao, J., and Zhang, Q. (2013). Characteristics of Ordovician Honghuayuan Paleokarst Reservoir in Kaili-Majiang-Danzhai Area, Southeastern Guizhou. *Mar. Oil-Gas Geol.* 18, 33–38.
- Dan, Y., Liang, B., Cao, J., Hao, Y., and Li, J. (2015). Characteristics and Solution Intensity of Karst Formations in Ordovician Carbonates in the Halahatang Area of the Northern Tarim Basin. *Exp. Pet. Geol.* 37, 582–590.
- Dan, Y., Lu, B., Liang, B., Zhang, Q., and Li, J. (2018). Effects of Paleozoic Carbonate Rock on Shale Gas Accumulation and Exploitation in Southern China. *Carsologica Sin.* 37, 343–350. doi:10.11932/karst20180304
- Du, J., Ye, X., Shi, S., and Wu, C. (2021). Technological Innovation and Achievements in the Exploration and Development of Shale Gas in Complex Mountainous Areas: A Case Study of the Zhaotong National Shale Gas Demonstration Area. *Nat. Gas. Ind.* 41, 41–50.
- Fahad, I. S., Salem, A., Temoor, M., Amirmasoud, K. D., and Shahin, N. (2021). Smart Shale Gas Production Performance Analysis Using Machine Learning Applications. *Pet. Res.* 7, 1–11. doi:10.1016/j.ptlrs.2021.06.003
- Fang, Z. (2019). Challenges and Countermeasures for Exploration and Development of Normal Pressure Shale Gas in Southern China. *Reserv. Eval. Dev.* 9, 1–13. doi:10.13809/j.cnki.cn32-1825/te.2019.05.001
- Gao, Y., Cai, X., He, X., Ding, A., Gao, H., Wu, Y., et al. (2021). Challenges and Development Direction of Experimental Testing Technology for Shale Gas Exploration and Development. *Reserv. Eval. Dev.* 11, 30–41. doi:10.13809/j.cnki.cn32-1825/te.2021.02.004
- Huang, X. (2012). *Cambrian Karst and Karst Water Environmental Characteristics and its Suitability with Tunnel Engineering in Yunnan-Guizhou area[D]*. Chengdu: Chengdu University of Technology. Available at: <https://kns.cnki.net/kcms/detail/detail.aspx?FileName=1012499746.nh&DbName=CMFD2013>.
- Jia, A., Wei, Y., and Jin, Y. (2016). Progress in Key Technologies for Evaluating Marine Shale Gas Development in China. *Pet. explor. Dev.* 43 (06), 949–955.
- Jiang, F., Pang, X., Ouyang, X., Guo, J., Jin, C., Huo, Z., et al. (2012). The Main Progress and Problems of Shale Gas Study and the Potential Prediction of Shale Gas Exploration. *Earth Sci. Front.* 19, 198–211.
- Karst Research Group, Institute of Geology, Chinese Academy of Sciences (1979). *Karst Research in China*. Beijing: Science Press, 20–21.
- Ladevèze, P., Rivard, C., Lavoie, D., Séjourné, S., Lefebvre, R., and Bordeleau, G. (2019). Fault and Natural Fracture Control on Upward Fluid Migration: Insights from a Shale Gas Play in the St. Lawrence Platform, Canada. *Hydrogeol. J.* 27, 121–143. doi:10.1007/s10040-018-1856-5
- Li, C., Rao, S., Hu, S., Wang, J., Wei, Z., Huang, Q., et al. (2017). Present Day Geothermal Field of the Jiaoshiba Shale Gas Area in Southeast of the Sichuan Basin, SW China. *Chin. J. Geophys.* 60, 617–627.
- Li, G., Luo, K., and Shi, D. (2020). Key Technologies, Engineering Management and Important Suggestions of Shale Oil/gas Development: Case Study of a Duvernay

FUNDING

This study was financially supported by the National Natural Science Foundation of China (grant no. 42172175) and China Geological Survey Projects (grant no. DD20179012, DD20190723, DD20221658).

ACKNOWLEDGMENTS

We would like to thank the Institute of Karst Geology, China Geological Survey, for providing data and allowing the publication of this article.

- Shale Project in Western Canada Sedimentary Basin. *Petroleum Explor. Dev.* 47, 791–802. doi:10.1016/s1876-3804(20)60094-5
- Liang, X., Xu, Z., Zhang, J., Zhang, Z., Li, Z., Jiang, P., et al. (2020). Key Efficient Exploration and Development Technologies of Shallow Shale Gas: A Case Study of Taiyang Anticline Area of Zhaotong. *Acta Pet. Sin.* 41, 1033–1048.
- Liss, W. E. (2014). Impacts of Shale Gas Advancements on Natural Gas Utilization in the United States. *Energy Technol.* 2, 953–967. doi:10.1002/ente.201402061
- Liu, N., and Wang, G. (2016). Shale Gas Sweet Spot Identification and Precise Geo-Steering Drilling in Weiyuan Block of Sichuan Basin, SW China. *Petroleum Explor. Dev.* 43, 1067–1075. doi:10.1016/s1876-3804(16)30124-0
- Liu, X.-W., Guo, Z.-Q., Liu, C., and Liu, Y.-W. (2017). Anisotropy Rock Physics Model for the Longmaxi Shale Gas Reservoir, Sichuan Basin, China. *Appl. Geophys.* 14, 21–30. (China: Sichuan Basin)(English). doi:10.1007/s11770-017-0609-x
- Ma, X., and Xie, J. (2018). The Progress and Prospects of Shale Gas Exploration and Exploitation in Southern Sichuan Basin, NW China. *Pet. explor. Dev.* 45, 161–169. doi:10.1016/s1876-3804(18)30018-1
- Ma, Z., Dan, Y., Chen, H., and Zhou, H. (2011). Sequence Stratigraphy and Paleogeography of Carboniferous in the South of Guizhou Sag, China. *J. Chengdu Univ. Technol. Nat. Sci. Ed.* 38 (05), 494–499.
- Ma, Y., Cai, X., and Zhao, P. (2018). China's Shale Gas Exploration and Development: Understanding and Practice. *Pet. explor. Dev.* 45 (04), 561–574. doi:10.1016/s1876-3804(18)30065-x
- Mao, J., Gu, S., and Zhang, Q. (1999). Framework of Fault Tectonics in Youjiang—Nanpanjiang Rift. *Geol. Guizhou* 03, 188–194.
- Miao, B. (2018). Study on Shale Gas Accumulation Conditions and Selection Evaluation of Carboniferous Dawuba Formation in South Guizhou. *Pet. Geol. Eng.* 32, 5–8.
- Sarkar, P., Singh, K. H., Ghosh, R., and Singh, T. N. (2018). Estimation of Elastic Parameters, Mineralogy and Pore Characteristics of Gondwana Shale in Eastern India for Evaluation of Shale Gas Potential. *Curr. Sci.* 115, 710–720. doi:10.18520/cs/v115/i4/710-720
- Soeder, D. J. (2018). The Successful Development of Gas and Oil Resources from Shales in North America. *J. Petroleum Sci. Eng.* 163, 399–420. doi:10.1016/j.petrol.2017.12.084
- Tang, X., Qin, W., Qin, Q., Gao, W., and Luo, S. (2014). Upper Paleozoic Group Shale Gas Resources Analysis in Southwestern Guizhou Province. *China Natl Admin. Coal Geol.* 26, 1–4.
- Wang, J., Luo, H., Liu, H., Lin, J., Li, L., and Lin, W. (2016). Influences of Adsorption/desorption of Shale Gas on the Apparent Properties of Matrix Pores. *Petroleum Explor. Dev.* 43, 158–165. doi:10.1016/s1876-3804(16)30019-2
- Wu, H. (2003). Discussion on Tectonic Palaeogeography of Nanpanjiang Sea in the Late Palaeozoic and Triassic. *J. Palaeogeogr.* 01, 63–76.
- Xu, Z., Yao, G., Guo, Q., Chen, Z., Dong, Y., Wang, P., et al. (2010). Genetic Interpretation about Geotectonics and Structural Transfiguration of the Southern Guizhou Depression. *Geotect. Metallog.* 34, 20–31. doi:10.16539/j.dgzyckx.2010.01.002
- Yu, X., Bian, J., and Liu, C. (2022). Determination of Energy Release Parameters of Hydraulic Fracturing Roof Near Goaf Based on Surrounding Rock Control of Dynamic Pressure Roadway. *J. Min. Strata Control. Eng.* 4, 013016. doi:10.13532/j.jmsce.cn10-1638/td.20210908.001

- Yuan, K., Wang, K., Gong, S., Qin, Y., Lu, S., Chen, R., et al. (2018). Shale Gas Enrichment Features and Impacting Factors in Carboniferous Dawuba Formation, Southern Guizhou Area. *China Natl. admin. Coal Geol.* 30, 28–34.
- Zeng, Q., Chen, S., He, P., Yang, Q., Guo, X., Chen, P., et al. (2018). Quantitative Prediction of Shale Gas Sweet Spots Based on Seismic Data in Lower Silurian Longmaxi Formation, Weiyuan Area, Sichuan Basin, SW China. *Petroleum Explor. Dev.* 45, 422–430. doi:10.1016/S1876-3804(18)30047-8
- Zhang, B., Yao, L., Luo, S., Zhao, Y., and Sun, W. (2016). Current Status and Outlook of Shale Gas Exploration and Development in Guizhou Province. *Nat. Gas. Technol. Econ.* 10, 57–59.
- Zhang, J. (2010). *The Research of Tectonic Evolution in Southern Guizhou depression*[D]. Qingdao: China University of Petroleum. Available at: <https://kns.cnki.net/kcms/detail/detail.aspx?FileName=2010281032.nh&DbName=CMFD2011>.
- Zhang, K., Jia, P., Wang, X., Jiang, Z., Song, Y., Jiang, L., et al. (2020a). Effect of Organic Maturity on Shale Gas Genesis and Pores Development: A Case Study on Marine Shale in the Upper Yangtze Region, South China. *Open Geosci.* 12, 1617–1629. doi:10.1515/geo-2020-0216
- Zhang, K., Jia, C., Song, Y., Jiang, S., Jiang, Z., Wen, M., et al. (2020b). Analysis of Lower Cambrian Shale Gas Composition, Source and Accumulation Pattern in Different Tectonic Backgrounds: A Case Study of Weiyuan Block in the Upper Yangtze Region and Xiuwu Basin in the Lower Yangtze Region. *Fuel* 263, 115978. doi:10.1016/j.fuel.2019.115978
- Zhang, K., Song, Y., Jiang, Z., Yuan, Z., Wang, X., Han, F., et al. (2022a). Research on the Occurrence State of Methane Molecules in Post-mature Marine Shales-A Case Analysis of the Lower Silurian Longmaxi Formation Shales of the Upper Yangtze Region in Southern China. *Front. Earth Sci.* 10 864279. doi:10.3389/feart.2022.864279
- Zhang, K., Song, Y., Jia, C., Jiang, Z., Han, F., Wang, P., et al. (2022b). Formation Mechanism of the Sealing Capacity of the Roof and Floor Strata of Marine Organic-Rich Shale and Shale Itself, and its Influence on the Characteristics of Shale Gas and Organic Matter Pore Development. *Mar. Pet. Geol.* 140, 105647. doi:10.1016/j.marpetgeo.2022.105647
- Zhao, J., Wang, Y., Yan, H., Ding, Y., Li, G., and Wang, N. (2021). Research on Prediction Method of Shale Reservoir Geochemical Parameters Based on Coal Field Logging Data. *Prog. Geophys.* 36, 2143–2150.
- Zou, C., Dong, D., Wang, Y., Li, X., Huang, J., Wang, S., et al. (2015). Shale Gas in China: Characteristics, Challenges and Prospects (I). *Petroleum Explor. Dev.* 42, 753–767. doi:10.1016/s1876-3804(15)30072-0
- Zou, C., Dong, D., Wang, Y., Li, X., Huang, J., Wang, S., et al. (2016). Shale Gas in China: Characteristics, Challenges and Prospects (II). *Petroleum Explor. Dev.* 43, 182–196. doi:10.1016/s1876-3804(16)30022-2
- Conflict of Interest:** The authors declare that the research was conducted in the absence of any commercial or financial relationships that could be construed as a potential conflict of interest.
- Publisher's Note:** All claims expressed in this article are solely those of the authors and do not necessarily represent those of their affiliated organizations, or those of the publisher, the editors, and the reviewers. Any product that may be evaluated in this article, or claim that may be made by its manufacturer, is not guaranteed or endorsed by the publisher.
- Copyright © 2022 Hu, Liu, Tan, Dan, He, Xiao and Li. This is an open-access article distributed under the terms of the Creative Commons Attribution License (CC BY). The use, distribution or reproduction in other forums is permitted, provided the original author(s) and the copyright owner(s) are credited and that the original publication in this journal is cited, in accordance with accepted academic practice. No use, distribution or reproduction is permitted which does not comply with these terms.